Cellular Physiology and Biochemistry

Cell Physiol Biochem 2026;60:518-529
DOI: 10.33594/000000886
Published online: 3 September 2026
Accepted: 17 July 2026

Published by Cell Physiol Biochem Press GmbH&Co. KG, Duesseldorf
www.cellphysiolbiochem.com

Original Paper

Mechanistic Insights into the Anticancer Effects of Homeopathic Arsenicum Iodatum: Apoptosis Induction, Cell-Cycle Arrest, and Caspase Activation in A549 Lung Cancer Cells

Vinu Krishnan[a,b] Manju Sreeranganathan[c]

[a]Homoeopathic Cancer Centre, Government of Kerala, [b]Vinayaka Mission Research Foundation, Salem, Tamil Nadu, [c]Department of Homeopathy, Government of Kerala

Key Words
Homeopathy • *Arsenicum iodatum* • A549 cells • Apoptosis • Lung cancer • Caspase activation • G_2/M arrest

Abstract
Background/Aims: Homeopathic medicines, including *Arsenicum iodatum*, have attracted increasing interest as potential adjunctive approaches in cancer research. However, the cellular mechanisms underlying their reported biological effects remain poorly understood. This study investigated the effects of homeopathic *Arsenicum iodatum* on apoptosis, cell cycle progression, and caspase activation in A549 human lung adenocarcinoma cells. ***Methods:*** A549 cells were treated with *Arsenicum iodatum* potencies (6C, 12C, 30C, and 200C). Apoptosis and cell cycle distribution were assessed by flow cytometry, while Caspase-7 and Caspase-9 activities were determined using indirect ELISA to evaluate the involvement of the intrinsic apoptotic pathway. ***Results:*** All tested potencies increased apoptotic cell populations compared with the control groups. The most pronounced biological effects were observed at the 30C and 200C potencies. These higher potencies were also associated with increased Caspase-7 and Caspase-9 activities, suggesting activation of the intrinsic apoptotic pathway. Vehicle-treated cells exhibited only minimal changes, indicating that the observed effects were not attributable to the solvent alone. ***Conclusion:*** Homeopathic *Arsenicum iodatum* induced measurable apoptosis-associated and cell cycle-related changes in A549 cells, accompanied by increased caspase activity. The strongest responses were observed at the 30C and 200C potencies. These findings suggest the involvement of intrinsic apoptotic signaling and warrant further mechanistic investigation. As this study represents an exploratory *in vitro* analysis, validation in additional experimental models and independent biological systems is required before broader conclusions can be drawn.

Dr Vinu Krishnan
Chief Medical Officer, Department of Homeopathy, Vinayaka Mission Research Foundation, Malappuram, Kerala, India
E-Mail Id: drvinukrishnanmd@gmail.com
ORCID ID: 0009-0000-3431-9536

Introduction

Lung cancer (LC) remains one of the leading causes of cancer-related morbidity and mortality worldwide. Approximately 85% of all diagnosed cases are classified as non-small cell lung cancer (NSCLC). Despite substantial advances in chemotherapy, radiotherapy, targeted therapies, and immunotherapy, patients with advanced or treatment-resistant disease continue to face limited therapeutic options and frequently experience considerable treatment-related toxicity. These challenges have stimulated increasing interest in complementary therapeutic approaches that may improve symptom control, enhance quality of life, or potentially modulate tumor biology while producing minimal adverse effects [1, 2].

Among these approaches, homeopathy has attracted attention following clinical observations reporting disease stabilization, reduced symptom burden, and prolonged progression-free survival in selected cancer patient cohorts. Nevertheless, despite these clinical findings, there remains a substantial lack of mechanistic evidence regarding the biological effects of highly diluted homeopathic preparations on cancer cells [3].

Arsenicum iodatum, a classical homeopathic remedy historically used for respiratory, inflammatory, and neoplastic disorders, has shown encouraging clinical observations in patients with lung cancer, including individuals with advanced disease or without actionable molecular targets [4]. These observations raise an important scientific question: can ultra-high dilutions of Arsenicum iodatum induce measurable, reproducible, and biologically relevant effects in lung cancer cells under controlled experimental conditions?

To address this question, the present study investigated the effects of homeopathic Arsenicum iodatum at four commonly used potencies (6C, 12C, 30C, and 200C) using the A549 human lung adenocarcinoma cell line as an *in vitro* model. Because tumor progression is closely associated with dysregulated apoptosis, altered cell-cycle progression, and impaired activation of intrinsic cell death pathways, the study focused on evaluating apoptosis induction, G_2/M cell-cycle arrest, and activation of the intrinsic apoptotic machinery.

Flow cytometry was employed to quantify apoptosis and analyze DNA content-based cell-cycle distribution, while indirect ELISA was used to determine Caspase-7 and Caspase-9 activity as indicators of intrinsic apoptotic pathway activation. Vehicle-treated controls were included throughout the experiments to distinguish potential treatment-specific effects from solvent-related changes.

The primary objective of this study was to evaluate the apoptosis-associated effects of homeopathic Arsenicum iodatum across different homeopathic potencies by examining its influence on apoptosis, cell-cycle regulation, and caspase activation in A549 human lung adenocarcinoma cells. Given the ongoing scientific debate regarding the biological plausibility of ultra-high dilutions and the challenges associated with experimental reproducibility, the present work should be regarded as an exploratory *in vitro* investigation. Rather than providing definitive evidence of efficacy, it aims to determine whether measurable cellular responses can be detected under well-controlled laboratory conditions and to provide a foundation for future mechanistic studies.

Materials and Methods

Study Design and Experimental Groups

The apoptosis-associated effects of homeopathic *Arsenicum iodatum* at four centesimal potencies (6C, 12C, 30C, and 200C) were evaluated using A549 human lung adenocarcinoma cells. All preparations were supplied in the standard homeopathic ethanol vehicle. Untreated cells served as the negative control, while vehicle-treated cells containing the corresponding ethanol concentration but lacking *Arsenicum iodatum* served as solvent controls.

To rigorously exclude solvent-related effects, vehicle-treated cells received the same final ethanol concentration (0.1% v/v) as the treatment groups and were exposed for the same duration (24 h). Vehicle controls were processed identically to treated cells throughout cell culture, apoptosis assessment, cell-cycle analysis, and caspase assays.

Cell Culture and Treatment

A549 human lung adenocarcinoma cells were cultured in Dulbecco's Modified Eagle Medium (DMEM) supplemented with 10% fetal bovine serum (FBS) and antibiotic-antimycotic solution under standard culture conditions (37°C, 5% CO_2).

Cells were treated with *Arsenicum iodatum* potencies (6C, 12C, 30C, and 200C) or the corresponding vehicle control for 24 hours. Following treatment, cells were harvested for apoptosis analysis, cell-cycle profiling, and caspase activity assays.

Flow Cytometry

Cell-Cycle Analysis

Approximately 1×10^6 cells from each experimental group were washed with phosphate-buffered saline (PBS), fixed overnight in cold 70% ethanol, and subsequently stained using the Muse™ Cell Cycle Reagent containing propidium iodide (PI) and RNase. DNA-content analysis was performed using the Muse™ Cell Analyzer to quantify the distribution of cells in the G_0/G_1, S, and G_2/M phases of the cell cycle.

Apoptosis Analysis

Apoptosis was assessed using the Muse™ Annexin V & Dead Cell Kit according to the manufacturer's instructions. Annexin V-FITC and propidium iodide (PI) staining enabled discrimination between viable, early apoptotic, late apoptotic, and dead cells. Quantitative apoptosis profiles were generated for each treatment group and compared with untreated and vehicle-treated controls.

Caspase Activity Assay (Indirect ELISA)

Caspase-7 and Caspase-9 activities were determined using an indirect enzyme-linked immunosorbent assay (ELISA) to evaluate activation of the intrinsic apoptotic pathway. Protein-normalized cell lysates were immobilized on ELISA plates and incubated with primary antibodies directed against Caspase-7 or Caspase-9, followed by horseradish peroxidase (HRP)-conjugated secondary antibodies. Color development was terminated using 5 N HCl, and absorbance was measured at 415 nm. Caspase activity was expressed as Units/mg protein.

Statistical Analysis

All experiments were performed in biological triplicates (n = 3), and data are presented as mean ± standard deviation (SD). Flow cytometric analyses were performed using standardized gating strategies to quantify viable, early apoptotic, late apoptotic, and dead-cell populations, while cell-cycle distribution was determined by DNA-content analysis. Caspase-7 and Caspase-9 activities were measured by indirect ELISA.

Statistical comparisons among groups were performed using one-way analysis of variance (ANOVA), followed by Dunnett's multiple comparison test, using the untreated control as the primary reference group. Where appropriate, matched vehicle-treated controls were included to distinguish treatment-specific effects from solvent-associated responses. Statistical significance was defined as $p < 0.05$.

Results

The effects of homeopathic Arsenicum iodatum on apoptosis, cell-cycle distribution, and caspase activation were investigated in A549 human lung adenocarcinoma cells following treatment with the 6C, 12C, 30C, and 200C potencies. Flow cytometric analyses included untreated control cells (Figs. 1 and 2), cells treated with 6C (Figs. 3 and 4), 12C (Figs. 5 and 6), 30C (Figs. 7 and 8), and 200C (Figs. 9 and 10), as well as vehicle-treated controls (Figs. 11 and 12). Overall, all tested potencies induced a shift from viable toward apoptotic cell populations, with the most pronounced biological responses observed following treatment with the 30C and 200C potencies.

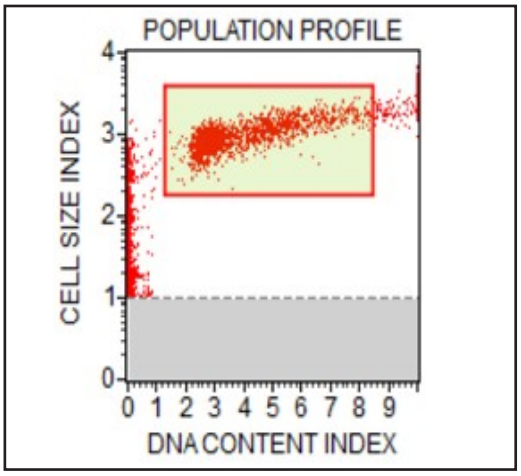

Fig. 1. Population profile of untreated control cells.

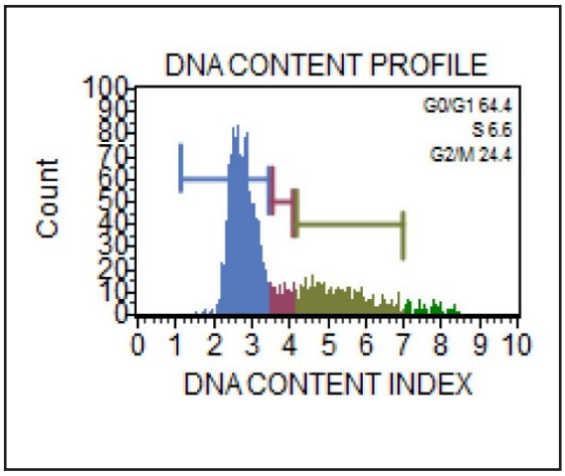

Fig. 2. DNA content profile of untreated control cells.

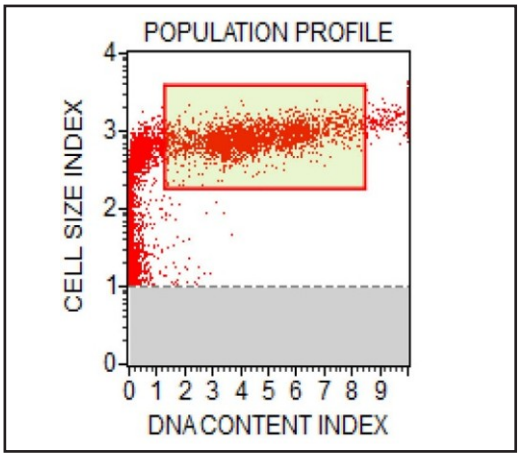

Fig. 3. Population profile of cells treated with 6C.

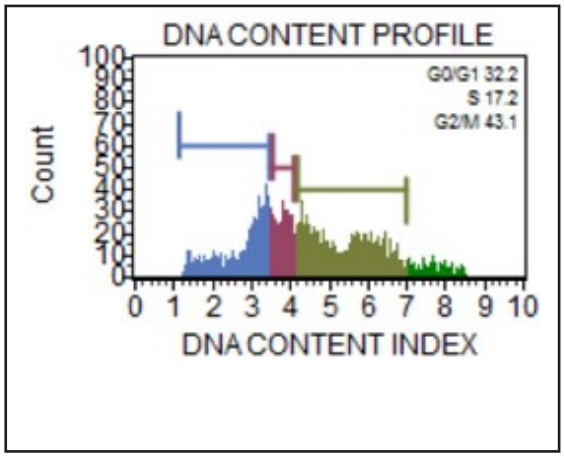

Fig. 4. DNA content profile of cells treated with 6C.

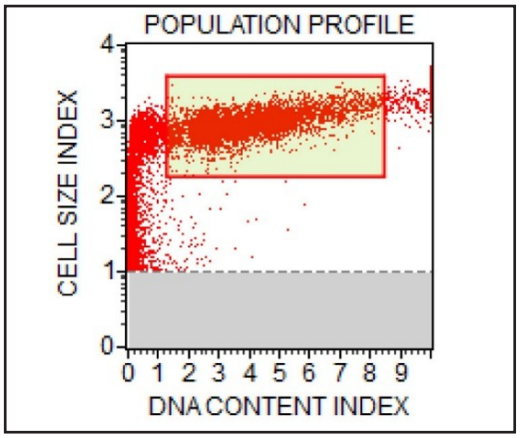

Fig. 5. Population profile of cells treated with 12C.

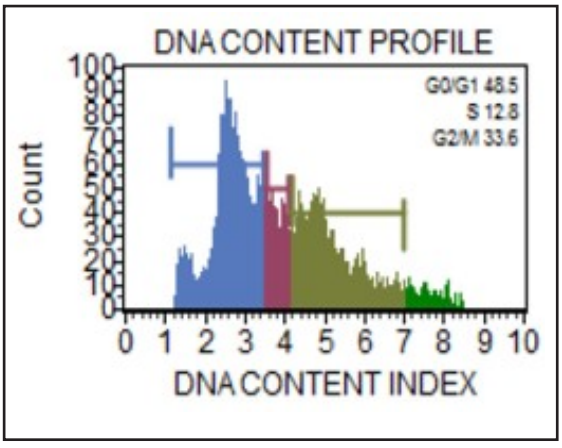

Fig. 6. DNA content profile of cells treated with 12C.

Table 1 and Figs. 1 and 2 summarize the baseline profile and cell-cycle distribution of untreated A549 cells. Most cells were in the G_0/G_1 phase (64.4%), whereas 6.6% were in S

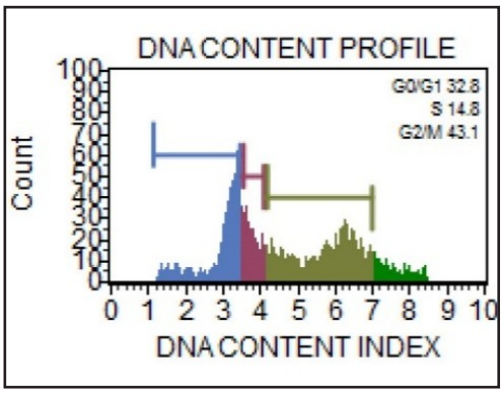

Fig. 7. Population profile of cells treated with 30C.

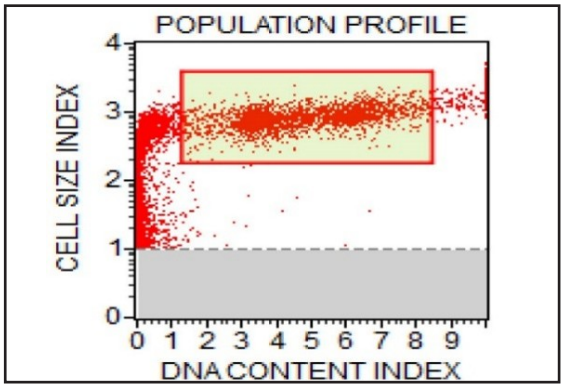

Fig. 8. DNA content profile of cells treated with 30C.

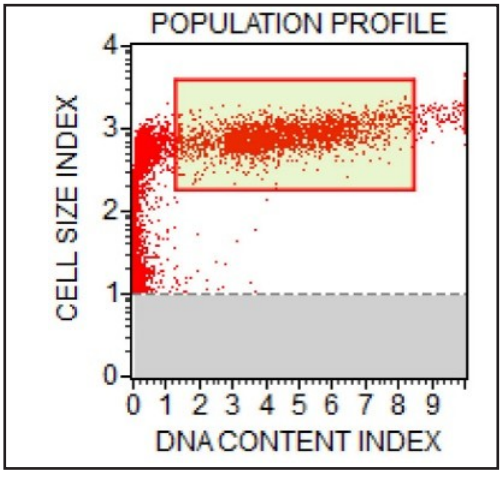

Fig. 9. Population profile of cells treated with 200C.

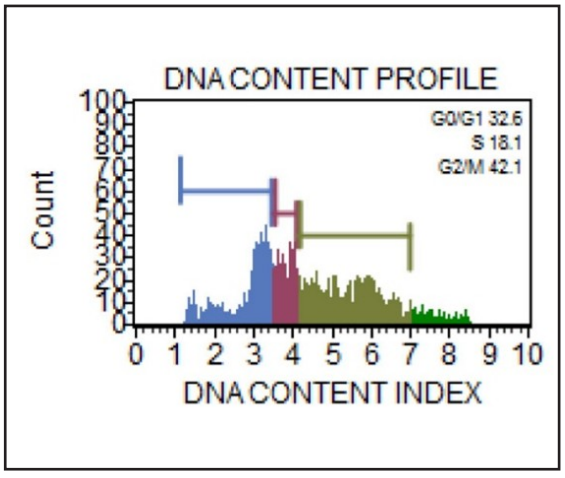

Fig. 10. DNA content profile of cells treated with 200C.

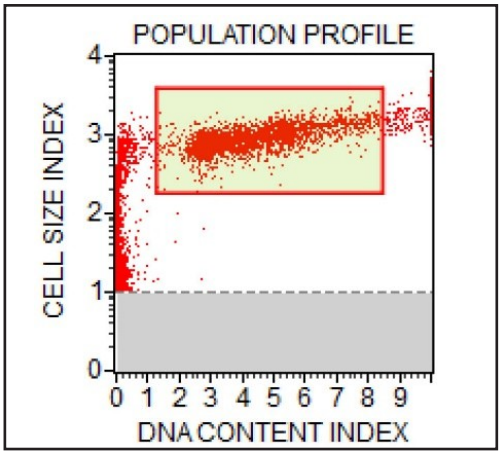

Fig. 11. Population profile of vehicle-treated cells.

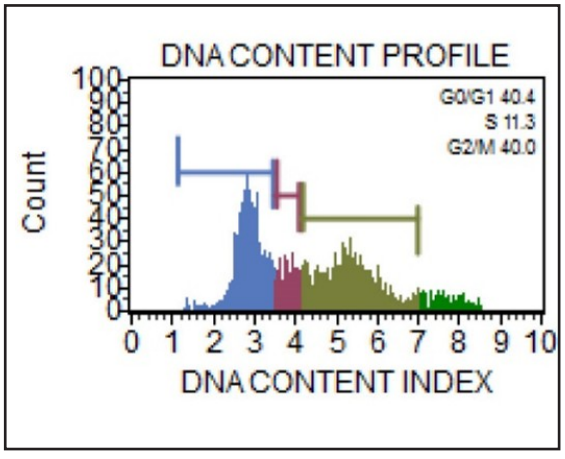

Fig. 12. DNA content profile of vehicle-treated cells.

phase and 24.4% in the G_2/M phase, representing the expected distribution of proliferating untreated cells. Mean fluorescence intensity and coefficient of variation (%CV) values were within the expected range for healthy A549 cultures.

As shown in Table 2 and Figs. 3 and 4, treatment with Arsenicum iodatum 6C reduced the proportion of cells in the G_0/G_1 phase while increasing both the S-phase and G_2/M populations. The G_2/M fraction increased to 43.1%, indicating marked alteration of cell-cycle progression compared with untreated controls.

Table 3 and Figs. 5 and 6 demonstrate that treatment with the 12C potency resulted in moderate alterations in cell-cycle distribution. Compared with untreated controls, the proportion of cells in G_0/G_1 decreased, whereas both S-phase and G_2/M populations increased, with 33.6% of cells accumulating in the G_2/M phase.

As summarized in Table 4 and Figs. 7 and 8, treatment with the 30C potency resulted in marked G_2/M accumulation (43.1%), accompanied by a reduction in the G_0/G_1 population and a moderate increase in S-phase cells. These findings indicate pronounced alterations in cell-cycle progression following treatment with the 30C potency.

Table 1. Cell-cycle distribution and fluorescence parameters of untreated control A549 cells

Parameter	G0/G1	S Phase	G2/M	Debris
% Gated	64.4	6.6	24.4	68.7
Mean Fluorescence	2744.3	3804.0	5315.8	631.0
% CV	11.7	5.0	13.9	368.9

Table 2. Cell-cycle distribution parameters of A549 cells treated with Arsenicum iodatum 6C

Parameter	G0/G1	S Phase	G2/M
% Gated	32.2	17.2	43.1
Mean Fluorescence	2735.2	3818.2	5384.7
% CV	24.1	4.8	14.9

Table 3. Cell-cycle distribution parameters of A549 cells treated with Arsenicum iodatum 12C

Parameter	G0/G1	S Phase	G2/M
% Gated	48.5	12.8	33.6
Mean Fluorescence	2606.5	3801.5	5153.5
% CV	20.5	4.8	14.3

Table 4. Cell Cycle Distribution of A549 Cells (30C)

Cell Cycle Phase	% Gated	Mean Fluorescence Intensity	% CV
G0/G1	32.8%	2892.1	21.2
S Phase	14.8%	3776.2	4.9
G2/M	43.1%	5682.6	14.5

Similarly, Table 5 and Figs. 9 and 10 show that treatment with the 200C potency produced marked G_2/M accumulation (42.1%), together with reduced G_0/G_1 and increased S-phase fractions. Overall, the cell-cycle distribution observed after 200C treatment was comparable to that produced by the 30C potency.

Table 6 and Figs. 11 and 12 summarize the effects of the vehicle control. Vehicle-treated cells exhibited moderate alterations in cell-cycle distribution compared with untreated controls, including a reduction in the G_0/G_1 fraction and moderate accumulation of cells in the G_2/M phase (40.0%). However, these changes remained less pronounced than those observed following treatment with the active Arsenicum iodatum potencies.

Direct comparison with the matched vehicle-control group demonstrated that the biological effects observed following Arsenicum iodatum treatment exceeded solvent-associated background responses. Although the ethanol vehicle induced moderate alterations in cell-cycle distribution, particularly G_2/M accumulation, treatment with the 30C and 200C potencies produced more pronounced apoptotic changes, greater G_2/M accumulation, and increased Caspase-7 and Caspase-9 activities.

Caspase-7 and Caspase-9 Activity

The effects of Arsenicum iodatum on activation of the intrinsic apoptotic pathway were further evaluated by measuring Caspase-7 and Caspase-9 activities using indirect ELISA.

Table 7 and Fig. 13 summarize Caspase-7 activity following treatment with the different potencies. Compared with untreated controls, Caspase-7 activity increased progressively across the treatment groups, with the highest activity observed in the 30C and 200C groups. One-way ANOVA demonstrated significant differences among treatment groups for Caspase-7 activity ($p < 0.001$). Dunnett's post hoc analysis revealed significantly increased activity in the 30C and 200C groups compared with untreated controls. Fig. 13 illustrates the progressive increase in Caspase-7 activity across the tested Arsenicum iodatum potencies, with the strongest responses observed following treatment with 30C and 200C.

Table 5. Cell-cycle distribution parameters of A549 cells treated with Arsenicum iodatum 200C

Parameter	G0/G1	S Phase	G2/M
% Gated	32.6	18.1	42.1
Mean Fluorescence	2790.4	3824.2	5411.7
% CV	22.7	4.7	14.2

Table 6. Cell-cycle distribution parameters of A549 cells treated with vehicle control

Parameter	G0/G1	S Phase	G2/M
% Gated	40.4	11.3	40.0
Mean Fluorescence	2820.5	3817.1	5306.8
% CV	14.3	4.9	13.0

Similarly, Table 8 and Fig. 14 summarize Caspase-9 activity. Caspase-9 activity increased across the treatment groups, with the greatest activity observed following treatment with the 30C and 200C potencies, whereas vehicle-treated cells exhibited only minimal changes relative to untreated controls. Significant overall group differences were observed by one-way ANOVA ($p < 0.001$), with the strongest increases detected following treatment with the 30C and 200C potencies. Fig. 14 illustrates this pattern, showing increased Caspase-9 activity across the treatment groups and the highest values following treatment with 30C and 200C.

Table 7. Caspase-7 activity in A549 cells treated with different potencies of Arsenicum iodatum

Sample code	Absorbance at 415nm	Protein concentration	Activity Units/mg protein
Control	0.5023	0.7208	0.69687
Vehicle	0.5265	0.7352	0.71613
6C	0.5307	0.7315	0.72546
12C	0.5330	0.7085	0.75231
30C	0.6096	0.7203	0.84635
200C	0.7172	0.7507	0.95543

Table 8. Caspase-9 activity in A549 cells treated with different potencies of Arsenicum iodatum

Sample code	Absorbance at 415nm	Protein concentration	Activity Units/mg protein
Control	0.4852	0.7208	0.67314
Vehicle	0.5209	0.7352	0.70851
6C	0.5811	0.7315	0.79436
12C	0.5911	0.7085	0.83431
30C	0.6293	0.7203	0.87370
200C	0.6684	0.7507	0.89042

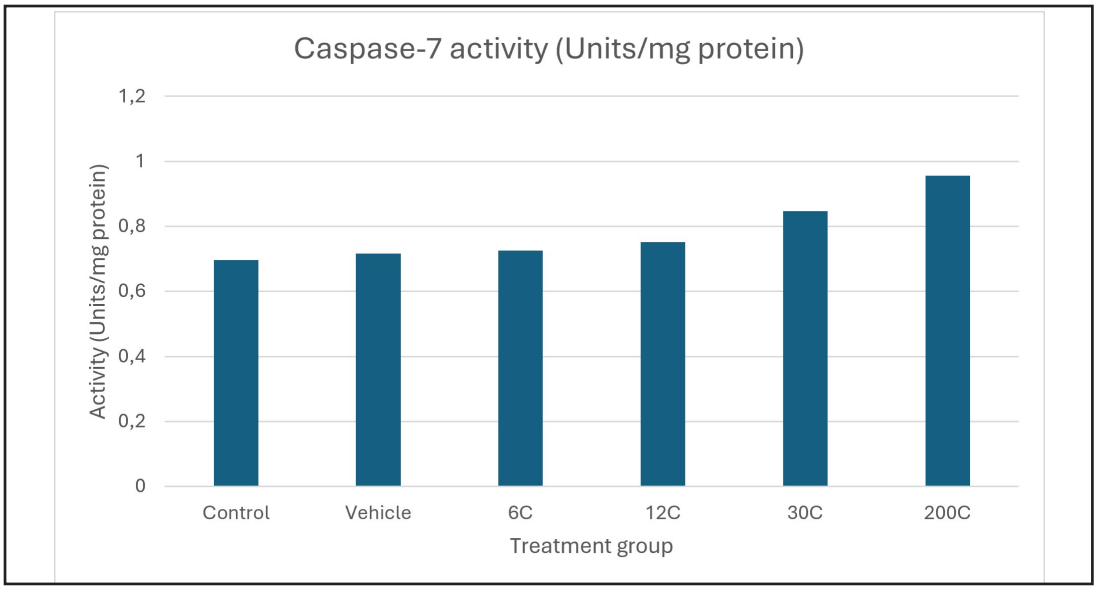

Fig. 13. Caspase-7 activity in A549 cells following treatment with different potencies of Arsenicum iodatum. Caspase-7 activity increased progressively, with the highest activity observed in the 30C and 200C treatment groups.

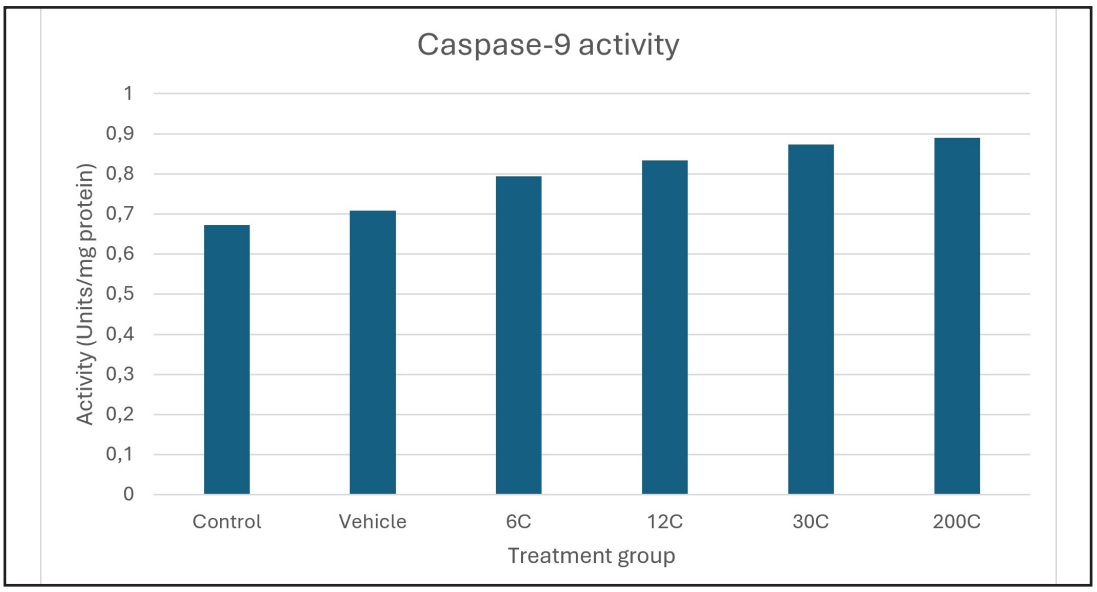

Fig. 14. Caspase-9 activity in A549 cells following treatment with different potencies of Arsenicum iodatum. Similar to Caspase-7, Caspase-9 activity increased progressively, with the strongest responses observed following treatment with the 30C and 200C potencies.

Discussion

The present study demonstrates that homeopathic Arsenicum iodatum induced measurable apoptosis-associated and cell-cycle-related alterations in A549 human lung adenocarcinoma cells. Flow cytometric analyses revealed increased apoptotic cell populations together with alterations in cell-cycle progression following treatment with all investigated potencies. Among the tested preparations, the 30C and 200C potencies consistently produced the most pronounced biological responses. These observations are consistent with previous reports indicating that G_2/M checkpoint arrest enhances cellular susceptibility to apoptosis by preventing mitotic progression and activating checkpoint-dependent cell death pathways [5]. The marked accumulation of cells in the G_2/M phase, particularly following treatment with the 30C and 200C potencies, is compatible with antiproliferative mechanisms described for several metal- and phytochemical-derived anticancer agents [6].

The observed increase in Caspase-7 and Caspase-9 activities further supports activation of the intrinsic apoptotic pathway. Caspase-9 functions as an initiator caspase within the mitochondrial apoptotic pathway, whereas Caspase-7 serves as an executioner caspase responsible for downstream apoptotic events. Their concurrent activation therefore suggests involvement of mitochondrial apoptotic signaling following Arsenicum iodatum treatment [7, 8]. Similar modulation of apoptotic signaling has previously been reported for several homeopathic preparations, including Arsenicum album, Carcinosinum, and Thuja occidentalis, in experimental cancer models [9, 11, 12].

The biological plausibility of ultra-high dilutions remains a matter of scientific debate. Nevertheless, recent nano-analytical investigations have suggested that homeopathic preparations may contain source-derived nanoparticles capable of interacting with biological systems and cellular signaling pathways [6, 10, 13, 14]. Although the precise mechanisms remain uncertain, the combined observations of apoptosis induction, G_2/M accumulation, and increased caspase activity reported in the present study suggest that Arsenicum iodatum may influence cellular pathways involved in growth regulation and programmed cell death. These findings should be regarded as preliminary evidence supporting further mechanistic investigation rather than definitive proof of therapeutic efficacy.

To further explore the biological relevance of the experimentally observed pathways, publicly available TCGA-LUAD and CPTAC datasets were analyzed using the UALCAN platform. Analysis of TCGA-LUAD data (Fig. 15) demonstrated significant dysregulation of several apoptosis- and cell-cycle-associated genes, including CASP7, CASP9, BAX, BCL2, CDKN1A, and CCNB1. In particular, CCNB1 showed marked overexpression in lung adenocarcinoma, consistent with dysregulated G_2/M cell-cycle control.

Protein-level analyses obtained from the CPTAC dataset (Fig. 16) demonstrated significant alterations in CASP7, CDKN1A, and CCNB1, whereas CASP9 did not exhibit statistically significant differences between normal and tumor tissues. Protein-expression data for BCL2 were not available within the analyzed CPTAC dataset.

Although these publicly available datasets do not directly validate the biological effects of Arsenicum iodatum, they provide independent biological context demonstrating that the pathways investigated experimentally in the present study are clinically relevant in human lung adenocarcinoma. The concordant transcriptomic and proteomic dysregulation observed for CASP7, CDKN1A, and CCNB1 further supports the relevance of apoptosis- and cell-cycle-associated signaling pathways in this disease.

Several limitations should be considered when interpreting the present findings. First, although untreated and vehicle-treated controls were included throughout all experiments, no established apoptosis-inducing positive control was incorporated. Future studies should therefore include reference compounds such as cisplatin, doxorubicin, or staurosporine to facilitate direct comparison of apoptosis induction, cell-cycle arrest, and caspase activation.

Second, the study was performed exclusively in a single A549 lung adenocarcinoma cell line. Validation in additional NSCLC cell lines, such as H1299 and H1975, together with non-malignant lung epithelial cells including BEAS-2B, will be important to determine the reproducibility, tumor selectivity, and broader biological relevance of the observed responses.

Third, the present investigation focused primarily on phenotypic cellular responses and did not evaluate upstream molecular regulators, including p53 signaling, mitochondrial membrane potential, reactive oxygen species generation, or checkpoint-associated proteins. Incorporation of these mechanistic endpoints in future studies would provide a more comprehensive understanding of the molecular pathways potentially involved.

Given the continuing scientific discussion surrounding high-dilution preparations, the present findings should be interpreted as preliminary and exploratory. They do not constitute definitive evidence of therapeutic efficacy or establish a specific molecular mechanism of action. Instead, the study demonstrates measurable cellular responses under controlled *in vitro* conditions and provides a rationale for further investigation using independent experimental systems, additional cancer models, and more comprehensive molecular analyses.

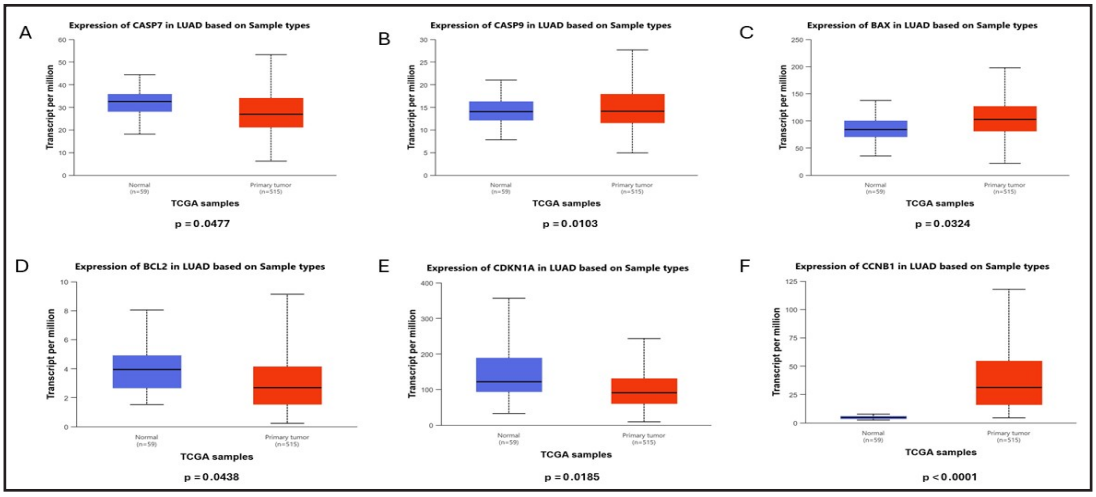

Fig. 15. Differential expression of apoptosis- and cell-cycle-associated genes in TCGA-LUAD.

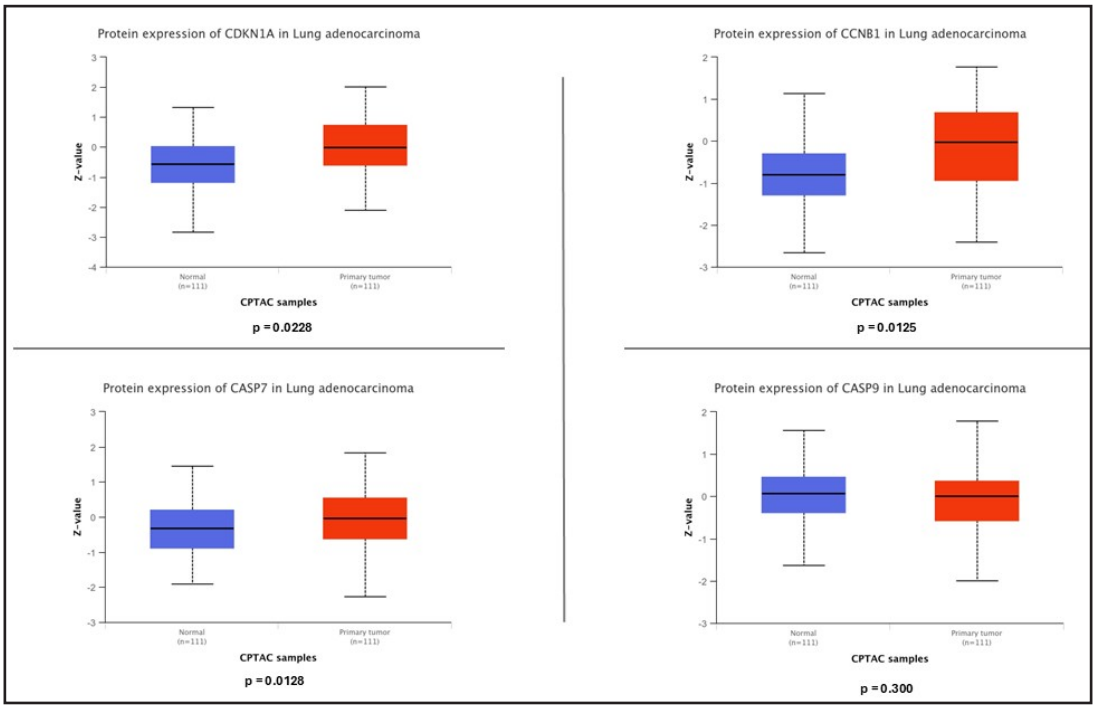

Fig. 16. CPTAC protein expression analysis.

Conclusion

The present exploratory *in vitro* study demonstrates that homeopathic *Arsenicum iodatum* induced measurable apoptosis-associated and cell-cycle-related changes in A549 human lung adenocarcinoma cells. All investigated potencies produced detectable biological responses, with the most pronounced effects consistently observed following treatment with the 30C and 200C potencies. These responses were characterized by increased apoptotic cell populations, enhanced G_2/M cell-cycle accumulation, and elevated Caspase-7 and Caspase-9 activities, suggesting activation of the intrinsic apoptotic pathway.

Vehicle-treated controls exhibited only limited cellular alterations, indicating that the observed biological responses were not attributable to solvent exposure alone. In addition, complementary analyses of publicly available TCGA-LUAD and CPTAC datasets demonstrated dysregulation of apoptosis- and cell-cycle-associated pathways in human lung adenocarcinoma, providing additional biological context for the experimental observations.

Although the precise mechanisms underlying the effects of ultra-high dilutions remain to be established, the present findings support further investigation of *Arsenicum iodatum* in experimental cancer models. Nevertheless, these results should be regarded as preliminary and exploratory. Validation in additional lung cancer cell lines, non-malignant control cells, independent experimental systems, and *in vivo* models, together with more comprehensive molecular analyses, will be required before broader biological or therapeutic conclusions can be drawn.

Acknowledgements

Author contributions

Vinu Krishnan (vk) did the conceptualization, methodology, investigation, experiments, supervision. Manju sreeranganathan (ms) did the data analysis,

interpretation, manuscript preparation, review and editing. All authors read the final manuscript and accepted.

Disclosure Statement

The authors have nothing to disclose.

References

1 Wahiduzzaman M, Ota A, Hosokawa Y. Novel mechanistic insights into the anti-cancer mode of arsenic trioxide. Current cancer drug targets. 2020 Feb 1;20(2):115-29.
2 Basu, N., Garg, M., Tandon, C., Das, B. C., & Tandon, S. (2023). Arsenicum album induces cell cycle arrest and apoptosis, and inhibits epithelial–mesenchymal transition in hormone-dependent MCF7 breast cancer cells. Homeopathy, 112(03), 160-169.
3 Pateriya, Anki. (2025). Arsenicum iodatum and arseicum album induces apoptosis and autophagy in glioblastoma multiforme. Bioinformation. 21. 4236-4240. 10.6026/973206300214236.
4 Khairul I, Wang QQ, Jiang YH, Wang C, Naranmandura H. Metabolism, toxicity and anticancer activities of arsenic compounds. Oncotarget. 2017 Apr 4;8(14):23905-23926. doi: 10.18632/oncotarget.14733. PMID: 28108741; PMCID: PMC5410354.
5 Jerard, C., Michael, B. P., Chenicheri, S., Vijayakumar, N., & Ramachandran, R. (2020). Rosmarinic acid–rich fraction induces G0/G1 arrest and apoptosis in cancer cells. Proceedings of the National Academy of Sciences, India Section B, 90, 515–522.
6 Bellavite, P., Signorini, A., Marzotto, M., Moratti, E., Bonafini, C., & Olioso, D. (2015). Cell sensitivity, non-linearity and inverse effects. Homeopathy, 104(2), 139–160. https://doi.org/10.1016/j.homp.2015.02.002
7 Elmore S. Apoptosis: a review of programmed cell death. Toxicol Pathol. 2007 Jun;35(4):495-516. doi: 10.1080/01926230701320337 PMID: 17562483; PMCID: PMC2117903.
8 Carneiro BA, El-Deiry WS. Targeting apoptosis in cancer therapy. Nature Reviews Clinical Oncology. 2020;17(7):395–417. doi:10.1038/s41571-020-0341-y.
9 Preethi K, Ellanghiyil S, Kuttan G, Kuttan R. Induction of apoptosis of tumor cells by some potentiated homeopathic drugs: implications on mechanism of action. Integr Cancer Ther. 2012 Jun;11(2):172-82 doi: 10.1177/1534735411400310. Epub 2011 Jul 19. PMID: 21771822.
10 Chikramane PS, Suresh AK, Kane SG, Bellare JR. Metal nanoparticle induced hormetic activation: a novel mechanism of homeopathic medicines. Homeopathy. 2017 Aug;106(3):135-144. doi: 10.1016/j.homp.2017.06.002. Epub 2017 Jul 21. PMID: 28844286.
11 Sunila, E & Thayele Purayil, Hamsa & Kuttan, Girija. (2011). Effect of Thuja occidentalis and its polysaccharide on cell-mediated immune responses and cytokine levels of metastatic tumor-bearing animals. Pharmaceutical biology. 49. 1065-73. 10.3109/13880209.2011.565351.
12 Pal A, Das S, Basu S, Kundu R. Apoptotic and autophagic death union by Thuja occidentalis homeopathic drug in cervical cancer cells with thujone as the bioactive principle. J Integr Med. 2022 Sep;20(5):463-472. doi: 10.1016/j.joim.2022.06.004. Epub 2022 Jun 15. PMID: 35752587.
13 Neelima Konduri, Anita Thyagarajan, Ravi P. Sahu. Anticancer Effects of Arsenic Compounds in Non-Small Cell Lung Cancer [JJ]. Diseases&Research, 2024, 4(2): 87-96. DOI: 10.54457/DR.202402003
14 Otto T, Sicinski P. Cell cycle proteins as promising targets in cancer therapy. Nature Reviews Cancer. 2017;17(2):93–115. doi:10.1038/nrc.2016.138.